Chapter 6

Dynamics of Prey-predator Model with Strong and Weak Allee Effect in the Prey with Gestation Delay [1]

6.1 Introduction

Prey-predator relationship is a very dominant phenomenon that occurs in nature. It has been an issue of attention among ecologists and biologists since last few decades. First model on prey-predator interaction is formulated and proposed by Lotka and Volterra. It contains a pair of first-order, nonlinear differential equations frequently used to describe the dynamics of biological systems in which two species interact. After that several attempts have been made to generalize and extend these equations.

A general two dimensional model of interaction between prey and predator is represented by

$$\frac{dx}{dt} = xf(x) - yg(x,y), \quad \frac{dy}{dt} = y(-d + cg(x,y)),$$

where x and y denote prey and predator densities at time t, respectively. $f(x)$ is per capita growth rate of prey. $g(x,y)$ and $cg(x,y)$ are functional and numerical response of predator for prey, where c $(0 < c < 1)$ stands for conversion coefficient denoting the number of newly born predators for each captured prey. d is mortality rate of predator population.

One vital factor of the prey-predator interaction is the intake rate of prey by a predator i.e. functional response. It helps to predict about a prey-predator dynamics with more accuracy. There are many types of functional response: Holling type I-III, Ratio dependent, Beddington-DeAngelis, Crowley-Martin, Hassel-Verley. Holling type I-III functional responses are prey dependent whereas Beddington-DeAngelis, Crowley-Martin, Hassel-Verley are prey and predator dependent i.e. functional response is function of both the prey and predator's density.

[1] A considerable part of this chapter is published in *Nonlinear Analysis: Modelling and Control*, **25**(3), 417-442, 2020.

Crowley-Martin [38] assumed that predation will decrease when the predator density is high due to interference among predators. Some investigations have been conducted on prey-predator model including Crowley-Martin functional response [38, 210, 136]. This type of response function is written as:

$$\eta(x,y) = \frac{\alpha x}{(1+ax)(1+by)},$$

where α, a and b are positive parameters denoting attack rate, handling time and magnitude of interference among predators, respectively.

The effect of intraspecific interference among predators has been investigated in prey-predator model with Holling type II functional response in [241, 205], with Holling type III functional response in [69], with Beddington-DeAngelis type functional response in [159, 117].

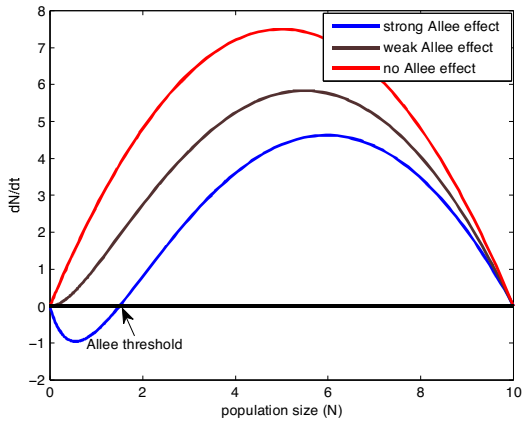

Fig. 6.1: Plot of per capita growth rate as a function of population size.

Allee effect plays a major role in the structure of population. It creates the possibilities of extinction of species [185, 241] and has a huge impact in population dynamics [4]. The Allee effect can be classified into two types on the basis of per capita growth rate at low density. These are known as strong Allee effect and weak Allee effect. Strong Allee effect have negative per capita growth rate at low population level and implies the existence of a threshold level of population so that the species become extinct below this level. Recently, Verma and Misra [216] have studied the impact of a constant prey refuge on the dynamics of a ratio-dependent predator-prey system with strong Allee effect in prey growth. They found that if prey refuge is less than the Allee threshold, the incorporation of prey refuge increases the threshold value of the predation rate and conversion efficiency at which unconditional extinction occurs. They also vindicated that the species can be protected by creating safe zones in accordance with the Allee threshold. On the other hand in weak Allee effect, the per capita growth rate decreases but

remains positive at low population level. Sexual selection [18, 147], reduced mating efficiency [47] and alleviated foraging efficiency [17] are some other reasons to give rise to Allee effect. Figure 6.1 makes us more clear that initially, the per capita growth rate is negative in strong Allee effect (blue) while it remains positive in weak Allee effect (brown).

The Allee effects are observed in many natural species. For example, in plants [62, 72], insects [112], marine invertebrates [198], in birds and mammals [33]. Recently, many ecologists have paid attention to the Allee effect [30, 59, 63, 152, 160, 185, 200, 240]. Some crucial results have been investigated in [25, 241] via a comparative analysis of prey-predator system with and without Allee effect. Some studies have been conducted on strong Allee effect on prey-predator model [69, 159, 160]. Weak Allee effect has been well studied by ecologists [63, 182, 186]. Some researchers have found the natural evidence of weak Allee effect by experimental work on flour beetles of the genus *Tribolium* [4, 103, 211]. They have shown that the per capita growth of beetles reaches its maximum at a medium density and the rate is positive at low density. Hopf-bifurcation is an important tool which helps to understand the behavior of system. It gives us such a critical value of a parameter that the stability behavior of system is contrasty in both the sides of the critical value [63, 117]. Hopf-bifurcation analysis with Allee effect has been carried out in [20, 63, 161, 159].

Time delay occurs in every biological movement. A delay differential equation shows much more complicated behavior than an ordinary differential equation. Delay is capable to change the stability behavior of any system. Due to time lag in conversion of prey population to predator population (gestation delay), dynamics of system changes. The prey-predator population model with gestation delay [144, 27, 92, 20, 210, 136, 121] has been studied. Some authors [182, 186] have considered an eco-epidemiological model with weak Allee effect in prey-predator population. They have concluded that chaotic dynamics can be controlled by the Allee parameter. Further Biswal *et al.* [20] have applied gestation delay and observed that the system exhibits chaotic oscillation due to increase of the delay.

Some studies have been conducted with Allee effect including gestation delay [20, 19, 161, 159]. Li *et al.* [117] investigated the stability and Hopf-bifurcation of a delayed density dependent prey-predator system with Beddington-DeAngelis functional response. Pal and Mandal [159] analyzed a modified delayed Leslie-Gower prey-predator model with strong Allee effect and shown that delay is incapable to decrease the risk of extinction. A prey-predator model with Crowley-Martin functional response including prey refuge has been considered by Maiti *et al.* [136]. They also examined the effect of gestation delay on the dynamics of the system.

To the best knowledge of the authors, a comparative analysis between strong and weak Allee effect in a prey-predator model with Crowley-Martin type functional response and gestation delay has not been studied. The main motive of this chapter is to analyze the dynamical complexity of Allee effect in the prey-predator model, studied by Tripathi *et al.* [210] and

further to show the impact of gestation time delay on the dynamics of the system. Keeping all these in mind, we reconstruct the model described by Tripathi *et al.* [210] by incorporating strong and weak Allee effects. Then we introduce gestation delay in the predator population.

6.2 Model formulation

Tripathi *et al.* [210] have analyzed the dynamics of following density dependent non-linear mathematical model

$$\begin{aligned}
&\frac{dx}{dt} = x\Big(1-x-\frac{cy}{1+a_1x+b_1y+c_1xy}\Big),\\
&\frac{dy}{dt} = y\Big(-d-ey-\frac{fx}{1+a_1x+b_1y+c_1xy}\Big),\\
&x(0)=x_0 \;>\; 0,\; y(0)=y_0 \;>\; 0.
\end{aligned} \tag{6.1}$$

In this model prey population grows logistically and predator is survived only on the prey population. They follow Crowley-Martin functional response to hunt the prey population. $r, K, \alpha, a, b, \delta_0$ and δ_1 are positive constants representing intrinsic rate of prey, carrying capacity, capture rate, handling time, magnitude of interference among predators, natural death rate of predators and crowding effect, respectively.

Now at low and sparse population, prey exhibits strong Allee effect. Let θ_s be the Allee parameter and f an auxiliary parameter which shapes the Allee function. The prey-predator dynamics with strong Allee effect in prey population is governed by the following system:

$$\begin{aligned}
&\frac{dx}{dt} = rx\big(1-\frac{x}{K}\big)\Big(1-\frac{\theta_s+f}{x+f}\Big)-\frac{\alpha xy}{(1+ax)(1+by)},\\
&\frac{dy}{dt} = \frac{c\alpha xy}{(1+ax)(1+by)}-\delta_0 y-\delta_1 y^2,\\
&x(0)=x_0 \;>\; 0,\; y(0)=y_0 \;>\; 0.
\end{aligned} \tag{6.2}$$

On the other hand, the model with weak Allee effect is based on probability of successful mating of prey population. It is incorporated into the population growth model by multiplying the probability $P(x)$ with birth term of prey population, where $P(x)$ is the probability of successful mating for a female prey during the reproductive period and should follow the bellow criteria:

1 No mating occurs at zero population size, $P(0)$=0.

2 $P'(x) > 0$ i.e. if population size increases the probability of successful mating increases.

3 Mating is guaranteed when the population is sufficiently large, that is $P(x) \to 1$ as $x \to \infty$.

We consider the probability function as $P(x)=\frac{x}{\theta_w+x}$, $\theta_w>0$ (rectangular hyperbolic) [47, 182]. Thus the model (6.1) with weak Allee effect can be written as:

$$\begin{aligned}
&\frac{dx}{dt}=rx\Big(1-\frac{x}{K}\Big)\Big(\frac{x}{\theta_w+x}\Big)-\frac{\alpha xy}{(1+ax)(1+by)},\\
&\frac{dy}{dt}=\frac{c\alpha xy}{(1+ax)(1+by)}-\delta_0 y-\delta_1 y^2,\\
&x(0)=x_0>0,\ y(0)=y_0>0.
\end{aligned}\tag{6.3}$$

In real situation, the conversion of hunted prey into predators growth is not instantaneous process rather, there occurs a time lag for gestation of predator biomass. Therefore, we assume that the reproduction of predator population after hunting prey is arbitrated by a constant time lag, called gestation delay. In order to get the rich dynamics of the system, we introduce gestation delay τ_s and τ_w in model (6.2) and (6.3) respectively. Then model (6.2) takes the form

$$\begin{aligned}
&\frac{dx}{dt}=rx\Big(1-\frac{x}{K}\Big)\Big(1-\frac{\theta_s+f}{x+f}\Big)-\frac{\alpha xy}{(1+ax)(1+by)},\\
&\frac{dy}{dt}=\frac{c\alpha x(t-\tau_s)y(t-\tau_s)}{(1+ax(t-\tau_s))(1+by(t-\tau_s))}-\delta_0 y-\delta_1 y^2,
\end{aligned}\tag{6.4}$$

subject to the non-negative condition $x(\zeta)=\phi_1(\zeta)>0$, $y(\zeta)=\phi_2(\zeta)>0$, $\zeta\in[-\tau_s,0]$, where $\phi_i\in C([-\tau_s,0]\to R_+)$, $i=1,2$.

Similarly in the presence of gestation delay model (6.3) can be written as

$$\begin{aligned}
&\frac{dx}{dt}=rx\Big(1-\frac{x}{K}\Big)\Big(\frac{x}{x+\theta_w}\Big)-\frac{\alpha xy}{(1+ax)(1+by)},\\
&\frac{dy}{dt}=\frac{c\alpha x(t-\tau_w)y(t-\tau_w)}{(1+ax(t-\tau_w))(1+by(t-\tau_w))}-\delta_0 y-\delta_1 y^2,
\end{aligned}\tag{6.5}$$

subject to the non-negative condition $x(\chi)=\phi_3(\chi)>0$, $y(\chi)=\phi_4(\chi)>0$, $\chi\in[-\tau_w,0]$, where $\phi_i\in C([-\tau_w,0]\to R_+)$, $i=3,4$.

6.3 Dynamics of non-delayed systems

In this section, we will study the dynamics of the model (6.2) and model (6.3).

6.3.1 Positivity and boundedness of model system (6.2)

It is necessary to prove that the model is biologically well behaved before the detailed study. From model system (6.2), we can write

$$x(t) = x(0)e^{\left[\int_0^t \left\{r\left(1-\frac{x(s)}{K}\right)\left(\frac{x(s)-\theta_s}{x(s)+f}\right)-\frac{\alpha y(s)}{(1+ax(s))(1+by(s))}\right\}ds\right]},$$

$$y(t) = y(0)e^{\left[\int_0^t \left\{\frac{c\alpha x(s)}{(1+ax(s))(1+by(s))}-\delta_0-\delta_1 y(s)\right\}ds\right]},$$

which shows that all solutions remain within the first quadrant of the xy plane starting from an interior point.

In the following theorem, we show that all solutions of system (6.2) are bounded which refers that the model is biologically well behaved.

Theorem 6.3.1. *The set*

$$\Omega = \left\{(x,y) : 0 \le x \le K,\ 0 \le x + \frac{1}{c}y \le \frac{2rK}{\delta}\right\}$$

is a positive invariant set for all the solutions initiating in the interior of the positive quadrant, where $\delta = min\{r, \delta_0\}$.

Proof. From first equation of the model system (6.2)

$$\frac{dx}{dt} \le rx\left(1-\frac{x}{K}\right)\left(\frac{x-\theta_s}{x+f}\right) \le rx\left(1-\frac{x}{K}\right),$$

which yields

$$\limsup_{t\to\infty} x(t) \le K.$$

Now suppose $W(t) = x(t) + \frac{1}{c}y(t)$.
Then we have

$$\frac{dW}{dt} = \frac{dx}{dt} + \frac{1}{c}\frac{dy}{dt} = rx\left(1-\frac{x}{K}\right) - \frac{\delta_0}{c}y - \frac{\delta_1}{c}y^2 \le 2rK - \delta W,$$

where $\delta = min\{r, \delta_0\}$.
Hence it follows that

$$\limsup_{t\to\infty} W(t) \le \frac{2rK}{\delta}.$$

We also note that $\frac{dW}{dt} < 0$ if $W > \frac{2rK}{\delta}$. Hence all solutions of the system (6.2) point towards Ω. Thus, Ω is a positively invariant set and all the solutions of model (6.2) are bounded. □

6.3.2 Local stability and Hopf-bifurcation

In this subsection, first we will find out all feasible equilibrium points of system (6.2) and present all possibilities for interior equilibrium. Then a brief description on their local stability has been done and lastly the analysis of Hopf-bifurcation through local stability of the positive equilibrium has been carried out.

6.3.2.1 Existence of equilibrium points

The system (6.2) has following equilibrium points:

1 The trivial equilibrium point $E_0(0,0)$.

2 The axial equilibrium points $E_1(\theta_s,0)$ and $E_2(K,0)$.

3 The system (6.2) has a unique positive equilibrium point $E^*(x^*,y^*)$ if the following condition holds true:

$$\theta_s < \frac{\delta_0}{c\alpha - a\delta_0} < K. \tag{6.6}$$

Remark 6.3.1. *The number of positive equilibrium for the system (6.2) depends on values of parameters, which we have chosen. Several possibilities are depicted in Figure 6.2.*

6.3.2.2 Local stability analysis

To analyze the local stability behavior of the equilibria, whenever they exist, we compute the Jacobian matrix for the model system (6.2) and further this matrix is calculated at each of equilibria. Then using Routh-Hurwitz criteria, we get following results:

1 The equilibrium Point $E_0(0,0)$ is always asymptotically stable.

2 The equilibrium Point $E_1(\theta_s,0)$ is unstable.

3
- $E_2(K,0)$ is locally asymptotic stable if $c\alpha K < \delta_0(1+aK)$.
- $E_2(K,0)$ is saddle point having stable manifold along the $x-$axis and unstable manifold along the $y-$axis if $c\alpha K > \delta_0(1+aK)$.

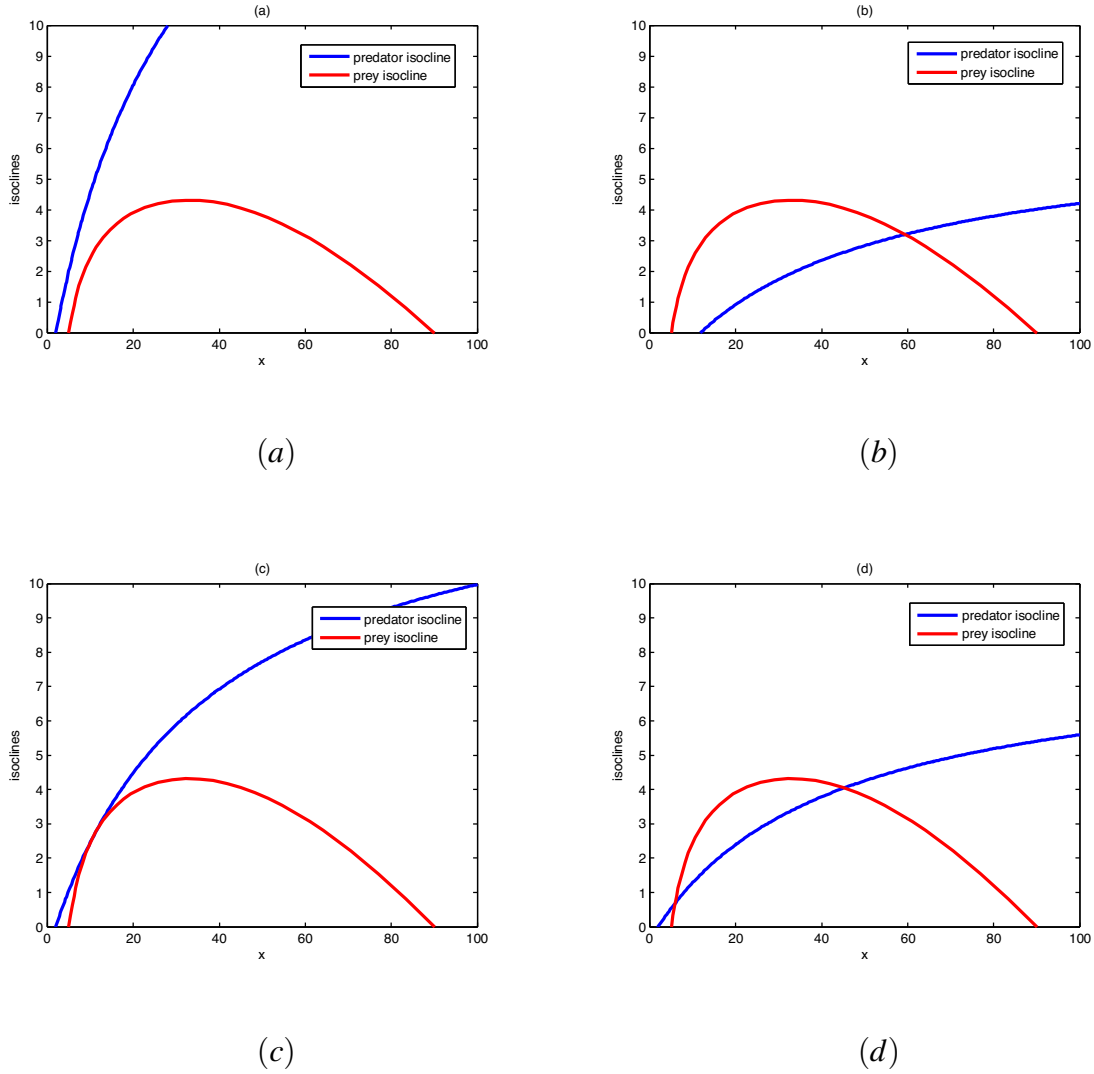

(a) (b)

(c) (d)

Fig. 6.2: Four possible relative of the prey and predator zero growth isoclines. (a) Interior equilibrium does not exist for the parametric values $\theta_s = 5,\ \delta_0 = 0.8\ , \delta_1 = 0.5$. (b-c) Interior equilibrium exists uniquely for the values of parameters $\theta_s = 5,\ \delta_0 = 4\ , \delta_1 = 2$ and $\theta = 5,\ \delta_0 = 0.8\ , \delta_1 = 1$ respectively. (d) Two interior equilibria for parameter values $\theta_s = 5,\ \delta_0 = 0.8\ , \delta_1 = 2$. Rest of the parameters are same as that in (6.15).

In order to investigate the stability behavior of positive equilibrium, let $M(E^*)$ denotes the variational matrix evaluated at E^*

$$M(E^*) = \begin{bmatrix} A_{11} & A_{12} \\ A_{21} & A_{22} \end{bmatrix},$$

where $A_{11} = -\frac{rx^*}{K}\left[\frac{x^*-\theta_s}{x^*+f} - \frac{(K-x^*)(f+\theta_s)}{(x^*+f)^2}\right] + \frac{\alpha a x^* y^*}{(1+ax^*)^2(1+by^*)}$, $A_{12} = -\frac{\alpha x^*}{(1+ax^*)(1+by^*)^2}$, $A_{21} = \frac{c\alpha y^*}{(1+ax^*)^2(1+by^*)}$, $A_{22} = -\frac{bc\alpha x^* y^*}{(1+ax^*)(1+by^*)^2} - \delta_1 y^*$.
Then the characteristic equation of $M(E^*)$ is given by

$$\lambda^2 + A_1\lambda + A_2 = 0, \tag{6.7}$$

where $A_1 = -tr(M(E^*)) = -(A_{11}+A_{22})$ and $A_2 = det(M(E^*)) = A_{11}A_{22} - A_{12}A_{21}$.

Using the Routh-Hurwitz criteria, both the eigenvalues of $M(E^*)$ have negative real part if and only if $A_1 > 0$, $A_2 > 0$. Thus, we can state the following theorem.

Theorem 6.3.2. *The system (6.2) is locally asymptotic stable around the interior equilibrium E^* if and only if $A_1 > 0$, $A_2 > 0$.*

Remark 6.3.2. *It can be noted that if $A_{11} < 0$, then $A_1 > 0$, $A_2 > 0$. Consequently the interior equilibrium E^* is asymptotically stable.*

In equation (6.7), if we assume $A_2 < 0$, then one eigenvalue is real and positive and other eigenvalue is real and negative. Thus, the following theorem follows:

Theorem 6.3.3. *If $A_2 < 0$, then the interior equilibrium E^* is a saddle point.*

Now, assume that $A_1 < 0$, and $A_2 > 0$. Then both the eigenvalues are real and positive or both the eigenvalues are complex conjugate having positive real parts. Thus we can state the following theorem.

Theorem 6.3.4. *If $A_1 < 0$, and $A_2 > 0$, then the interior equilibrium E^* is unstable.*

Remark 6.3.3. *We have seen that E_0 is always stable equilibrium and interior equilibrium E^* is stable if $A_{11} < 0$. Hence, if $A_{11} < 0$ holds, then system (6.2) exhibits bi-stability. Bi-stability is a phenomenon where the system can converge to different equilibrium in the same parametric region based on the variation of initial condition.*

6.3.2.3 Hopf-bifurcation analysis

Here auxiliary parameter f is an important parameter which shapes the Allee function. In this subsection, we analyze how the dynamics of system (6.2) changes with respect to f by using Hopf-bifurcation analysis.

Now, to show the existence of Hopf-bifurcation, we assume that $A_1 = 0$, $A_2 > 0$. This gives $f = f^*$, where f^* satisfies

$$\frac{rx^*}{K}\left[\frac{x^*-\theta_s}{x^*+f^*} - \frac{(K-x^*)(f^*+\theta_s)}{(x^*+f^*)^2}\right] - \frac{\alpha a x^* y^*}{(1+ax^*)^2(1+by^*)} + \frac{bc\alpha x^* y^*}{(1+ax^*)(1+by^*)^2} + \delta_1 y^* = 0, \tag{6.8}$$

and it leads us to the following theorem.

Theorem 6.3.5. *Assume that $f = f^*$ and $A_2 > 0$. Then system (6.2) has Hopf-bifurcation near the equilibrium point $E^*(x^*, y^*)$ if following condition is satisfied.*

$$(x^* - f^*)(K + \theta_s) + 2x^* f^* \neq 0.$$

Proof. At $f = f^*$, we have $tr(M(E^*)) = 0$ and $det(M(E^*)) > 0$,which shows the eigenvalues are purely imaginary and conjugate to each other at $f = f^*$. We also have

$$\frac{d}{df}[tr(M(E^*))]_{f=f^*} = \frac{rx^*}{K(x^*+f)^2}\left[(x^* - \theta_s) + \frac{(K-x^*)\{(x^*+f) - 2(f+\theta_s)\}}{(x^*+f)}\right]$$

$$= \frac{rx^*}{K(x^*+f)^2}[(x^* - f^*)(K + \theta_s) + 2x^* f^*].$$

Hence, the transversality condition holds under the condition

$$(x^* - f^*)(K + \theta_s) + 2x^* f^* \neq 0.$$

This shows that E^* changes its nature from locally asymptotic stable to unstable as parameter f crosses the critical value $f = f^*$. Therefore by the Hopf-bifurcation theorem, system (6.2) exhibits Hopf-bifurcation near the interior equilibrium point E^*. □

6.3.3 Dynamics of weak Allee effect model

The analysis of model (6.3) with weak Allee effect is similar to that of model (6.2) with strong Allee effect. Thus, in this section we omit the detail mathematical analysis and present the main results of this model system briefly.

1. All the solutions of model system (6.3) with initial conditions that initiate in R^2_+ are positive invariant and uniformly bounded.

2. The system (6.3) has following equilibrium points: $E_0(0,0)$, $E_2(K,0)$ and the unique interior equilibrium $E_*(x_*, y_*)$. E_* exists if the following condition holds:

$$0 < \frac{\delta_0}{c\alpha - a\delta_0} < K. \tag{6.9}$$

3. – The equilibrium point $E_0(0,0)$ is stable proper node.

- $E_2(K,0)$ is locally asymptotic stable if $c\alpha K < \delta_0(1+aK)$, and a saddle point having stable manifold along the $x-$axis and unstable manifold along the $y-$axis if $c\alpha K > \delta_0(1+aK)$.

4. In order to analyze the stability behavior of interior equilibrium, let $M'(E_*)$ denotes the variational matrix evaluated at E_*. Then

$$M'(E_*) = \begin{bmatrix} A'_{11} & A'_{12} \\ A'_{21} & A'_{22} \end{bmatrix},$$

where $A'_{11} = -\frac{rx_*}{K(\theta_w+x_*)}\left[x_* - \frac{\theta_w(K-x_*)}{(x_*+\theta_w)}\right] + \frac{\alpha a x_* y_*}{(1+ax_*)^2(1+by_*)}$, $A'_{12} = -\frac{\alpha x_*}{(1+ax_*)(1+by_*)^2}$, $A'_{21} = \frac{c\alpha y_*}{(1+ax_*)^2(1+by_*)}$, $A'_{22} = -\frac{bc\alpha x_* y_*}{(1+ax_*)(1+by_*)^2} - \delta_1 y_*$.

Then the characteristic equation of $M'(E_*)$ is given by

$$\lambda^2 + A'_1\lambda + A'_2 = 0,$$

where $A'_1 = -tr(M'(E_*)) = -(A'_{11}+A'_{22})$ and $A'_2 = det(M'(E_*)) = A'_{11}A'_{22} - A'_{12}A'_{21}$.

Using the Routh-Hurwitz criteria, we have

- The system (6.3) is locally asymptotic stable around the interior equilibrium E'_* if and only if $A'_1 > 0,\ A'_2 > 0$.
- It can be noted that if $A'_{11} < 0$, then the interior equilibrium E_* is locally asymptotically stable.

5. Now, to show the existence of Hopf-bifurcation we assume that $A'_1 = 0, A'_2 > 0$. This gives $\theta_w = \theta_w^*$, where

$$\frac{rx_*}{K(\theta_w^*+x_*)}\left[x_* - \frac{\theta_w^*(K-x_*)}{(x_*+\theta_w^*)}\right] - \frac{\alpha a x_* y_*}{(1+ax_*)^2(1+by_*)} + \frac{bc\alpha x_* y_*}{(1+ax_*)(1+by_*)^2} + \delta_1 y_* = 0.$$

Thus, we can state the following.

Theorem 6.3.6. *Assume that $\theta_w = \theta_w^*$, $A'_2 > 0$ and $x_* > \theta_w^*$. Then system (6.3) has Hopf-bifurcation near the equilibrium point $E_*(x_*, y_*)$.*

Now, we are in position to compare the system with strong Allee effect and weak Allee effect. In the Table 6.1, comparison between both the cases has been carried out.

Table 6.1: Comparative results for strong Allee (6.2) and weak Allee system (6.3).

S. No.	Strong Allee effect	Weak Allee effect
1	The per capita growth rate of prey population is negative.	The per capita growth rate of prey population is slower then without Allee effect but remains positive (see Fig.6.1).
2	The model (6.2) has locally asymptotically stable trivial equilibrium point. Consequently possibility of extinction is high at low population density.	Species always coexist if they initially exist under weak Allee effect (model (6.3)).
3	Model (6.2) shows bi-stability when E^* is locally asymptotically stable.	Model (6.3) never shows bi-stability. When interior equilibrium is unstable then populations fluctuate around it.
4	Model (6.2) does not show the Hopf-bifurcation with respect to Allee parameter θ_s.	Model (6.3) shows the Hopf-bifurcation with respect to Allee parameter θ_w.

6.4 Local stability and Hopf-bifurcation of delayed models

In this section, we will investigate local stability of the positive equilibrium E^* and exhibition of local Hopf-bifurcation. We know that delay does not affect the equilibrium of the system. Therefore equilibrium points are same as non-delayed model system. We omit the proof of the following theorem as it is similar to non-delayed system.

Theorem 6.4.1. *All the solutions of model system (6.4) and (6.5) with positive initial conditions are positive invariant and uniformly bounded.*

To see the effect of time delay on the dynamics of the system, we can re-write model system (6.4) as

$$\frac{dU(t)}{dt} = F(U(t), U(t-\tau_s)),$$

where $U(t) = [x(t), y(t)]^T$, $U(t-\tau_s) = [x(t-\tau_s), y(t-\tau_s)]^T$.

Let $x(t) = x^* + x'(t),\ y(t) = y^* + y'(t)$. Then linearizing system (6.4) about the interior equilibrium solution $E^*(x^*, y^*)$, we have

$$\frac{dZ}{dt} = PZ(t) + QZ(t-\tau_s),$$

where

$$P = \left(\frac{\partial F}{\partial U(t)}\right)_{E^*} = \begin{bmatrix} a_3 - a_1 & -a_2 \\ 0 & -a_4 \end{bmatrix},\ Q = \left(\frac{\partial F}{\partial U(t-\tau_s)}\right)_{E^*} = \begin{bmatrix} 0 & 0 \\ ca_1 & ca_2 \end{bmatrix},$$

$a_1 = \frac{\alpha y^*}{(1+ax^*)^2(1+by^*)},\ a_2 = \frac{\alpha x^*}{(1+ax^*)(1+by^*)^2},\ a_3 = r(1-\frac{2x^*}{K})(\frac{x^*-\theta_s}{x^*+f}) + rx^*(1-\frac{x^*}{K})\frac{(f+\theta_s)}{(x^*+f)^2},\ a_4 = \delta_0 + 2\delta_1 y^*$
and $Z(t) = [x'(t), y'(t)]^T$.

Thus, the variational matrix of the system (6.4) at E^* is given by

$$J = P + Qe^{-\lambda\tau_s} = \begin{bmatrix} a_3 - a_1 & -a_2 \\ ca_1 e^{-\lambda\tau_s} & ca_2 e^{-\lambda\tau_s} - a_4 \end{bmatrix}$$

and corresponding characteristic equation is

$$\lambda^2 + A\lambda + (B\lambda + C)e^{-\lambda\tau_s} + D = 0, \tag{6.10}$$

where $A = a_1 - a_3 + a_4,\ B = -ca_2,\ C = ca_2a_3$ and $D = a_4(a_1 - a_3)$.

Case (1): $\tau_s = 0$. Then characteristic equation becomes

$$\lambda^2 + (A+B)\lambda + (C+D) = 0. \tag{6.11}$$

Remark 6.4.1. *The characteristic equation is same as the characteristic equation (6.7) of the non-delayed model system (6.2) studied earlier.*

All the roots of characteristic equation (6.11) have negative real part if and only if $(H_1):\ A+B>0,\ C+D>0$.

Case (2): $\tau_s > 0$. Let $i\omega(\omega > 0)$ be a root of equation (6.10), then we have

$$-\omega^2 + Ai\omega + (Bi\omega + C)(\cos(\omega\tau_s) - i\sin(\omega\tau_s)) + D = 0.$$

On equating real and imaginary parts, we obtain

$$\begin{aligned} B\omega\sin(\omega\tau_s) + C\cos(\omega\tau_s) &= \omega^2 - D, \\ C\sin(\omega\tau_s) - B\omega\cos(\omega\tau_s) &= A\omega, \end{aligned} \tag{6.12}$$

which leads to

$$z^2 + pz + q = 0, \tag{6.13}$$

where $p = A^2 - B^2 - 2D$, $q = D^2 - C^2$ and $z = \omega^2$.
Let $f(z) = z^2 + pz + q$
(H_2): $p > 0$, $q > 0$.

Remark 6.4.2. *1. If (H_2) holds, then equation (6.13) has no positive roots. Hence, all the roots of (6.10) have negative real part and hence $E^*(x^*, y^*)$ is asymptotically stable for all $\tau_s \geq 0$ under conditions (H_1) and (H_2).*

2. If (H_1) fails and (H_2) holds true, then E^* is unstable for all $\tau_s \geq 0$.

$(H_3) : q < 0$.
If (H_1) and (H_3) hold, then equation (6.13) has a unique positive root ω_0^2. Substitution of ω_0 into equation (6.12) gives us

$$B\omega_0 \sin(\omega_0\tau_s) + C\cos(\omega_0\tau_s) = \omega_0^2 - D,$$

$$C\sin(\omega_0\tau_s) - B\omega_0\cos(\omega_0\tau_s) = A\omega_0,$$

which yields

$$\tau_{s_i} = \frac{1}{\omega_0}\cos^{-1}\left[\frac{C(\omega_0^2 - D) - AB\omega_0^2}{B^2\omega_0^2 + C^2}\right] + \frac{2i\pi}{\omega_0}\ ,\ i = 0, 1, 2\ldots\ . \tag{6.14}$$

(H_4) : $p < 0$, $q > 0$, $p^2 > 4q$.
If (H_1) and (H_4) hold, then equation (6.13) has two positive roots ω_1^2 and ω_2^2, substituting $\omega_{1,2}^2$ into equation (6.12), we have

$$\tau_{s_j}^{1,2} = \frac{1}{\omega_{1,2}}\cos^{-1}\left[\frac{C(\omega_{1,2}^2 - D) - AB\omega_{1,2}^2}{B^2\omega_{1,2}^2 + C^2}\right] + \frac{2j\pi}{\omega_{1,2}}\ ,\ j = 0, 1, 2\ldots\ .$$

Let $\lambda(\tau_s)$ be a root of equation (6.10) satisfying $Re\{\lambda(\tau_{s_i})\} = 0$. Then differentiating equation (6.10) with respect to τ_s, we obtain.

$$\left(\frac{d\lambda}{d\tau_s}\right)^{-1} = \frac{(2\lambda + A)e^{\lambda\tau_s}}{(B\lambda + C)\lambda} + \frac{B}{(B\lambda + C)\lambda} - \frac{\tau_s}{\lambda},$$

$$\left[\frac{d\lambda}{d\tau_s}\right]^{-1}_{\lambda = i\omega_0} = \frac{(2i\omega_0 + A)e^{i\omega_0\tau_s}}{(Bi\omega_0 + C)i\omega_0} + \frac{B}{(Bi\omega_0 + C)i\omega_0} - \frac{\tau_s}{i\omega_0},$$

$$Re\left[\frac{d\lambda}{d\tau_s}\right]^{-1}_{\lambda=i\omega_0} = \frac{-B\omega_0^2(A\cos(\omega_0\tau_s) - 2\omega_0\sin(\omega_0\tau_s)) + C\omega_0(2\omega_0\cos(\omega_0\tau_s) + A\sin(\omega_0\tau_s)) - B^2\omega_0^2}{B^2\omega_0^4 + C^2\omega_0^2},$$

where $\sin(\omega_0\tau_s)$ computed as

$$\sin(\omega_0\tau_s) = \frac{AC\omega_0 + B\omega_0(\omega_0^2 - D)}{B^2\omega_0^2 + C^2}.$$

After a little calculation, we obtain

$$Re\left[\frac{d\lambda}{d\tau_s}\right]^{-1}_{\lambda=i\omega_0} = \frac{f'(\omega_0^2)}{B^2\omega_0^2 + C^2}.$$

But $sign\left[\frac{d}{d\tau_s}Re(\lambda)\right]_{\lambda=i\omega_0} = sign\left[Re\left(\frac{d\lambda}{d\tau_s}\right)\right]_{\lambda=i\omega_0}$
$(H_5): f'(\omega_0^2) \neq 0.$

Hence $\left[\frac{d}{d\tau_s}Re(\lambda)\right]_{\lambda=i\omega_0} \neq 0$ under condition (H_5).

Now we are in position to state the following theorem.

Theorem 6.4.2. *For system (6.4), assume that (H_1), (H_3) and (H_5) hold. Then there exists a positive number τ_{s_0} such that the equilibrium E^* is locally asymptotically stable when $\tau_s < \tau_{s_0}$ and unstable when $\tau_s > \tau_{s_0}$. Furthermore system undergoes a Hopf-bifurcation at E^* when $\tau_s = \tau_{s_0}$.*

The investigation of local stability and Hopf-bifurcation for model (6.5) is similar. In the case of weak Allee effect in prey population. Let (H_1'), (H_3') and (H_5') are hypotheses for model system (6.5) corresponding to (H_1), (H_3) and (H_5) respectively.

Theorem 6.4.3. *For system (6.5), assume that (H_1'), (H_3') and (H_5') hold, there exists a positive number τ_{w_0} such that the equilibrium E_* is locally asymptotically stable when $\tau_w < \tau_{w_0}$ and unstable when $\tau_w > \tau_{w_0}$. Furthermore system exhibits a Hopf-bifurcation at E_* when $\tau_w = \tau_{w_0}$.*

6.5 Stability and direction of Hopf-bifurcation

In the previous section, we obtained the condition under which periodic solution bifurcates from the steady state at the critical value of τ_s. In this section, we will study the direction of Hopf-bifurcation and stability of the periodic solution by using normal form theory and center manifold theory introduced in Hassard *et al.* [80]. We assume that system (6.4) undergoes Hopf-bifurcation at the steady state E^* for $\tau_s = \tau_{s_0}$ and $\pm i\omega_0$ is corresponding purely imaginary roots of the characteristic equation at E^*.

Let $x_1(t) = x(t) - x^*$, $y_1(t) = y(t) - y^*$ and still denote $x_1(t)$, $y_1(t)$ by $x(t)$, $y(t)$. Let $\tau_s = \tau_{s_0} + \mu$, $\mu \in R$ so that Hopf-bifurcation occurs at $\mu = 0$, system (6.4) is transformed into

$$\frac{dx}{dt} = (a_3 - a_1)x(t) - a_2 y(t) + \sum_{i+j\geq 2} \frac{1}{i!j!} F_{ij}^{(1)} x^i(t) y^j(t),$$
$$\frac{dy}{dt} = ca_1 x(t-\tau_s) + ca_2 y(t-\tau_s) - a_4 y(t) + \sum_{i+j+l\geq 2} \frac{1}{i!j!l!} F_{ijl}^{(2)} x^i(t-\tau_s) y^j(t-\tau_s) y^l(t),$$

where

$$F^{(1)} = rx\left(1 - \frac{x}{K}\right)\left(\frac{x-\theta_s}{x+f}\right) - \frac{\alpha xy}{(1+ax)(1+by)},$$
$$F^{(2)} = \frac{c\alpha x(t-\tau_s)y(t-\tau_s)}{(1+ax(t-\tau_s))(1+by(t-\tau_s))} - \delta_0 y - \delta_1 y^2,$$
$$F_{ij}^{(1)} = \left[\frac{\partial^{i+j} F^{(1)}}{\partial x^i \partial y^j}\right]_{E^*}, \quad F_{ijl}^{(2)} = \left[\frac{\partial^{i+j+l} F^{(2)}}{\partial x^i(t-\tau_s)\partial y^j(t-\tau_s)\partial y^l}\right]_{E^*}.$$

Here, we omit the detailed analysis and write only the results, which are obtained. One can easily derive them by using the computation process similar to that in Song and Wei [195] and Tripathi *et al.* [210]. The standard results can be computed as:

$$c_1(0) = \frac{i}{2\omega_0\tau_{s_0}}\left(g_{20}g_{11} - 2|g_{11}|^2 - \frac{|g_{02}|^2}{3}\right) + \frac{g_{21}}{2}, \ \mu_2 = -\frac{Re\{c_1(0)\}}{Re\{\lambda'(\tau_{s_0})\}},$$

$$\beta_2 = 2Re\{c_1(0)\}, \ T_2 = -\frac{Im(c_1(0)) + \mu_2 Im(\lambda'(\tau_{s_0}))}{\omega_0\tau_{s_0}},$$

where g_{20}, g_{11}, g_{02} and g_{21} are evaluated as follows:

$$g_{20} = \frac{\tau_{s_0}}{\bar{d}}\left[F_{20}^{(1)} + 2\rho F_{11}^{(1)} + \bar{\rho}^*\left(e^{-2i\omega_0\tau_{s_0}} F_{200}^{(2)} + 2\rho e^{-2i\omega_0\tau_{s_0}} F_{110}^{(2)}\right)\right],$$

$$g_{11} = \frac{\tau_{s_0}}{\bar{d}}\left[F_{20}^{(1)} + 2Re\{\rho\}F_{11}^{(1)} + \bar{\rho}^*\left(F_{200}^{(2)} + 2Re\{\rho\}F_{110}^{(2)}\right)\right],$$

$$g_{02} = \frac{\tau_{s_0}}{\bar{d}}\left[F_{20}^{(1)} + 2\bar{\rho}F_{11}^{(1)} + \bar{\rho}^*\left(e^{2i\omega_0\tau_{s_0}} F_{200}^{(2)} + 2\bar{\rho}e^{2i\omega_0\tau_{s_0}} F_{110}^{(2)}\right)\right],$$

$$g_{21} = \frac{\tau_{s_0}}{\bar{d}}\Big[F_{11}^{(1)} W_{20}^{(2)}(0) + \bar{\rho}F_{11}^{(1)} W_{20}^{(1)}(0) + \bar{\rho}^*\Big(F_{110}^{(2)}\big(\bar{\rho}e^{i\omega_0\tau_{s_0}} W_{20}^{(1)}(-1) + e^{i\omega_0\tau_{s_0}} W_{20}^{(2)}(-1)$$
$$+ 2\rho e^{-i\omega_0\tau_{s_0}} W_{11}^{(1)}(-1) + 2e^{-i\omega_0\tau_{s_0}} W_{11}^{(2)}(-1)\big)\Big)\Big],$$

where

$$W_{20}(\theta) = \frac{ig_{20}}{\omega_0\tau_{s_0}} q(0) e^{i\omega_0\tau_{s_0}\theta} + \frac{i\bar{g}_{02}}{3\omega_0\tau_{s_0}} \bar{q}(0) e^{-i\omega_0\tau_{s_0}\theta} + E_1 e^{2i\omega_0\tau_{s_0}\theta},$$

$W_{11}(\theta) = -\frac{ig_{11}}{\omega_0\tau_{s_0}}q(0)e^{i\omega_0\tau_{s_0}\theta} + \frac{i\bar{g}_{11}}{\omega_0\tau_{s_0}}\bar{q}(0)e^{-i\omega_0\tau_{s_0}\theta} + E_2,$
$E_1 = (E_1^{(1)}, E_1^{(2)})^T \in R^2$ and $E_2 = (E_2^{(1)}, E_2^{(2)})^T \in R^2$ are constant vectors, computed as:

$$E_1 = 2\begin{bmatrix} 2i\omega_0 - a_3 + a_1 & a_2 \\ -ca_1e^{-2i\omega_0\tau_{s_0}} & 2i\omega_0 + a_4 - ca_2e^{-2i\omega_0\tau_{s_0}} \end{bmatrix}^{-1} \begin{bmatrix} F_{20}^{(1)} + 2\rho F_{11}^{(1)} + \rho^2 F_{02}^{(1)} \\ e^{-2i\omega_0\tau_{s_0}}F_{200}^{(2)} + 2\rho e^{-2i\omega_0\tau_{s_0}}F_{110}^{(2)} + \rho^2 e^{-2i\omega_0\tau_{s_0}}F_{020}^{(2)} - \delta_1\rho^2 \end{bmatrix},$$

$$E_2 = -2\begin{bmatrix} a_3 - a_1 & -a_2 \\ ca_1 & -a_4 + ca_2 \end{bmatrix}^{-1} \begin{bmatrix} F_{20}^{(1)} + 2Re\{\rho\}F_{11}^{(1)} + |\rho|^2 F_{02}^{(1)} \\ F_{200}^{(2)} + 2Re\{\rho\}F_{110}^{(2)} + |\rho|^2 F_{020}^{(2)} - \delta_1|\rho|^2 \end{bmatrix},$$

$$\rho = \frac{ca_1e^{-i\omega_0\tau_{s_0}}}{i\omega_0 + a_4 - ca_2e^{-i\omega_0\tau_{s_0}}}, \quad \rho^* = \frac{a_2}{i\omega_0 + ca_2e^{i\omega_0\tau_{s_0}} - a_4},$$
$$\bar{d} = 1 + \rho\bar{\rho}^* + c\bar{\rho}^*\tau_{s_0}(a_1 + \rho a_2)e^{-i\omega_0\tau_{s_0}}.$$

These expressions give a description of the bifurcating periodic solution in the center manifold of system (6.4) at critical values $\tau_s = \tau_{s_0}$ which can be stated as follows:

1. μ_2 determines the direction of Hopf-bifurcation. If $\mu_2 > 0 (< 0)$ then the Hopf-bifurcation is supercritical (subcritical).

2. β_2 determines the stability of bifurcated periodic solution. If $\beta_2 > 0 (< 0)$ then the bifurcated periodic solutions are unstable (stable).

3. T_2 determines the period of bifurcating periodic solution. The period increases (decreases) if $T_2 > 0 (< 0)$.

Remark 6.5.1. *We can also analyze the properties of bifurcating periodic solution for weak Allee case by adopting the same process.*

6.6 Numerical simulation

In this section, we will present numerical simulations to validate the analytical findings, obtained in previous sections using MATLAB R2017a.

6.6.1 Non-delayed models

For model (6.2), we consider a set of parameters as follows:

$$\begin{aligned} &r = 3,\ K = 90,\ \theta_s = \theta_w = 0.05,\ f = 0.002,\ \alpha = 0.7,\\ &a = 0.02,\ b = 0.03,\ c = 0.6,\ \delta_0 = 0.8,\ \delta_1 = 0.25, \end{aligned} \tag{6.15}$$

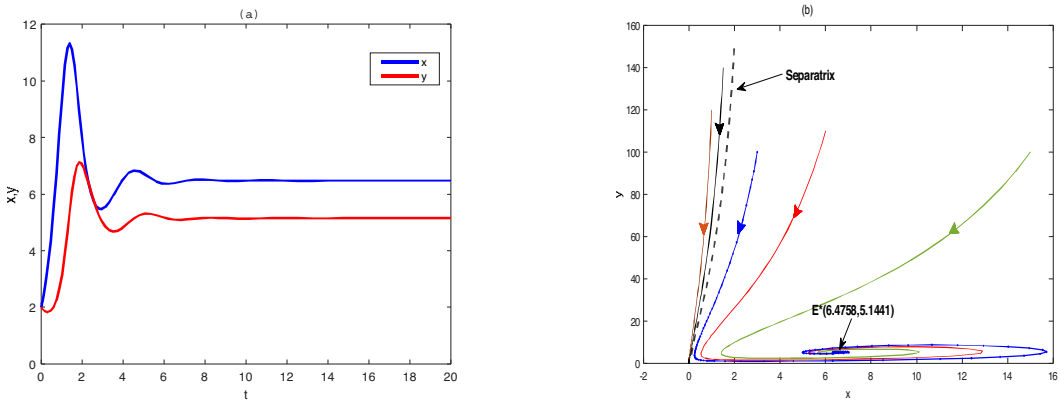

Fig. 6.3: (a) Time series of x and y, (b) Trajectories initiated from region of attraction of both the locally stable equilibrium points, system (6.2) shows bi-stability.

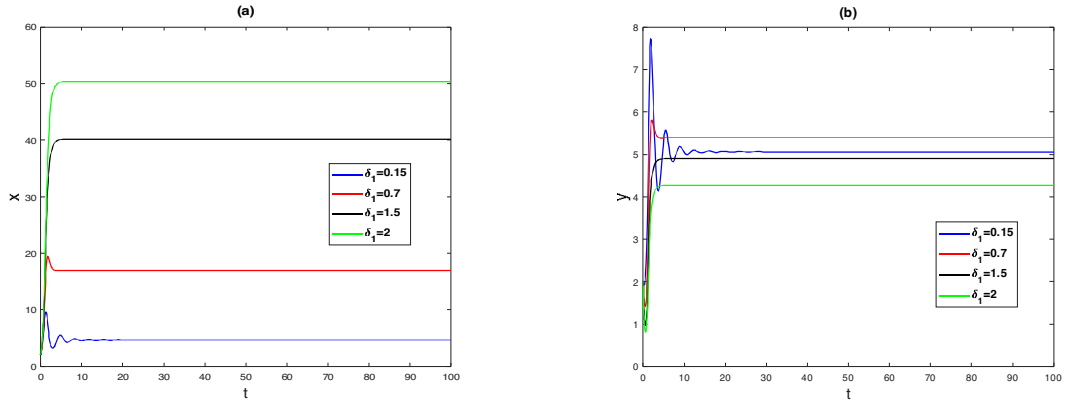

Fig. 6.4: Time series evolution of x and y for the different values of parameter δ_1.

6.6.1.1 Strong Allee effect

For the set of values of parameters in equation (6.15), condition (6.6) is satisfied. Thus, there exists a positive equilibrium $E^*(6.4758, 5.1441)$. It is also noted that $A_{11} < 0$ holds for the set of parameters chosen in (6.15). So the interior equilibrium E^* is asymptotically stable, depicted in Figure 6.3. This figure shows that the density of prey and predator species both are

increasing initially, then some fluctuations occur and eventually settle down to their respective steady states.

As the trivial equilibrium point E_0 is always asymptotically stable for system (6.2). Therefore, under the condition of stability of positive equilibrium E^*, system shows bi-stability. A separatrix lies in the $xy-$plane which divides the plane into two regions in such a way that trajectories starting from different regions approach to different steady states. This phenomenon of system (6.2) is depicted in Figure 6.3(b). From the figure, it is clear that solution curves, which are initiated from left of the separatrix, approach to $E_0(0,0)$ and solution curves, which are initiated from right of the separatrix, approach to interior equilibrium point E^*. The effect of parameter δ_1 on both the prey and predator species is shown in Figure 6.4. In Figure 6.4(a) and 6.4(b), time series analysis is shown for four different values of $\delta_1(\delta_1 = 0.15, 0.7, 1.5, 2)$. From Figure 6.4(a), it is noted that prey population increases with the parameter δ_1. The predator population initially grows up with δ_1 but after a threshold value of δ_1=$\delta_1^* = 0.825$ it starts to decrease and settles down at its equilibrium level (see Fig. 6.4(b)).

Now, we observe the dynamical behavior of the system for the variation of the Allee parameter θ_s. It is noted that as we increase the value of parameter θ_s, the time of fluctuations for both prey and predator increase. Time series analysis has been shown in Figure 6.5 for different values of θ_s, which refers that the system is stable for $\theta_s = 0.1, 0.5$ and 1. At $\theta_s \geq \theta_s^* = 1.4985$, interior equilibrium E^* becomes unstable and beyond this threshold value of θ_s, system converges to the stable trivial equilibrium point E_0. This shows that as we increase Allee parameter θ_s, the life expectancy of both biological species decreases and after a critical value of θ_s $(= \theta_s^*)$, they move to extinction.

In the model system (6.2), the auxiliary parameter f is also a crucial parameter because it shapes the Allee function. Therefore, we will analyze how the dynamics of system changes with respect to f by using Hopf-bifurcation analysis. The condition of Hopf-bifurcation, which is derived in Theorem 6.3.5, is satisfied. The critical value of parameter f where bifurcation occurs is calculated from equation (6.8) and it is $f = f^* = 3.22$. In Figure 6.3 we depicted time series (Fig. 6.3(a)) and phase portrait (Fig. 6.3(b)) for $f = 0.002 < f^* = 3.22$, which refers that the system (6.2) is stable. Figure 6.6 shows that the system is unstable for $f = 3.7 > f^* = 3.22$ and periodic solution occurs.

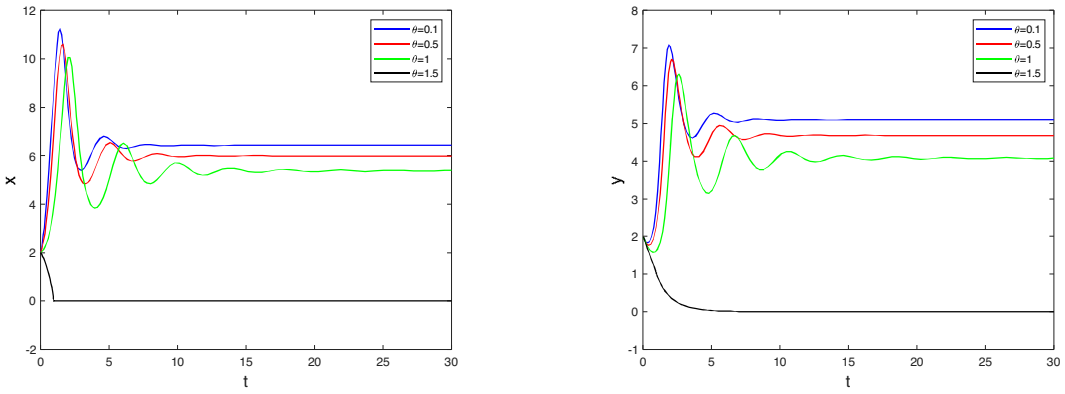

Fig. 6.5: Time series solutions of x and y for the different values of Allee parameter θ_s.

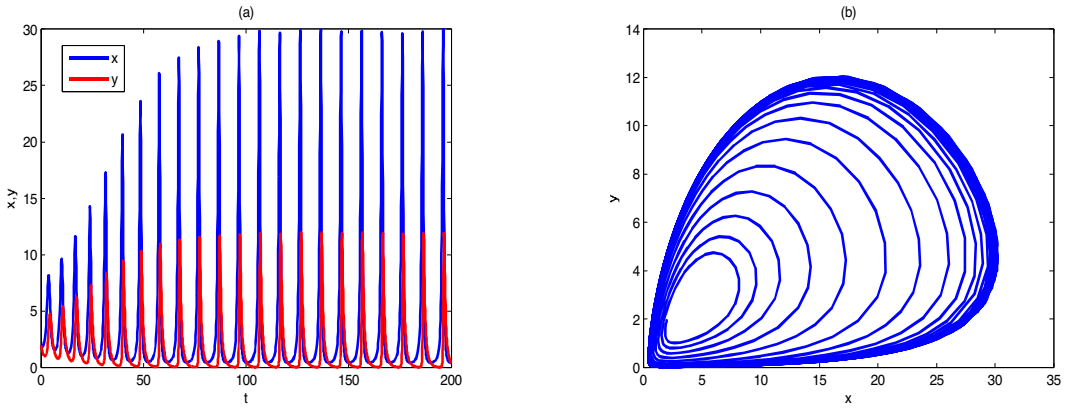

Fig. 6.6: Time evolution of species and existence of periodic solution when $f = 3.7 > f^*$.

6.6.1.2 Weak Allee effect

On the other hand for the system (6.3), with weak Allee effect in prey population and with same values of parameters as in (6.15), condition for the existence of unique equilibrium $E_*(x_*, y_*)$ is satisfied and it is given by $E_*(6.4782, 5.1464)$. The conditions of Theorem 6.3.6 are also satisfied. Therefore, Hopf-bifurcation with respect to θ_w occurs near the interior equilibrium E_*. The threshold value of θ_w is evaluated as $\theta_w^* = 3.36$. Thus the equilibrium point E_* is asymptotically stable for $\theta_w = 2.5 < \theta_w^*$ which is shown in Figure 6.7 and unstable for $\theta_w = 4.3 > \theta_w^*$ (fig. 6.8) and a periodic solution exists around E_*. The bifurcation diagram has been shown in Figure 6.9 by taking θ_w as a bifurcation parameter. This figure depicts the dynamics of the system as the Allee parameter increases. From the figure, it is clear that for $\theta_w < \theta_w^*$, the system (6.3) is stable but as θ_w crosses its critical value, the system loses its stability and undergoes Hopf-bifurcation.

We have drawn phase portrait for model (6.2) and (6.3) together in a single figure keeping all the values of parameters and initial pair same. Then both are compered with the model proposed by Tripathi *et al.* [210]. The significant difference can be seen among model with strong Allee effect, model with weak Allee effect and model with no Allee effect in the Figure 6.10. The figure shows that possibilities of extinction of species are high at low density under strong Allee effect whereas under weak Allee effect, both species coexist.

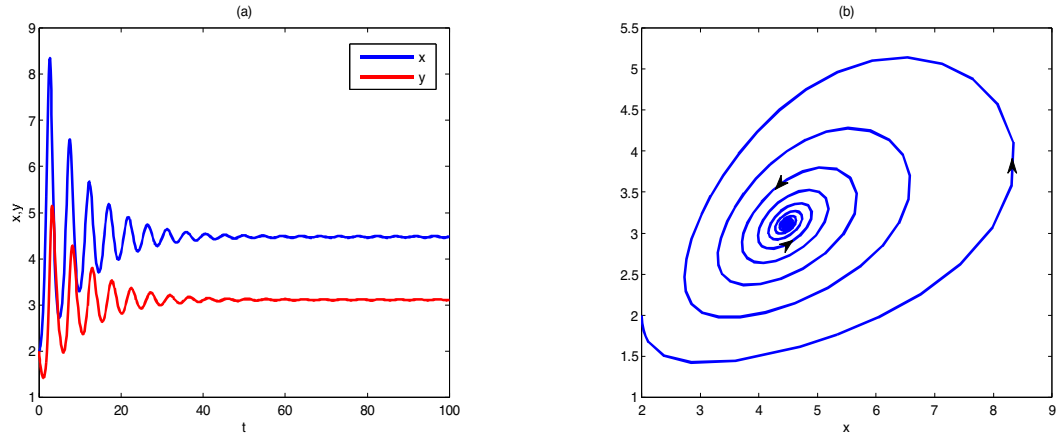

Fig. 6.7: (a) Time series of x and y, (b) phase portrait when $\theta_w = 2.5 < \theta_w^*$. E_* is asymptotically stable.

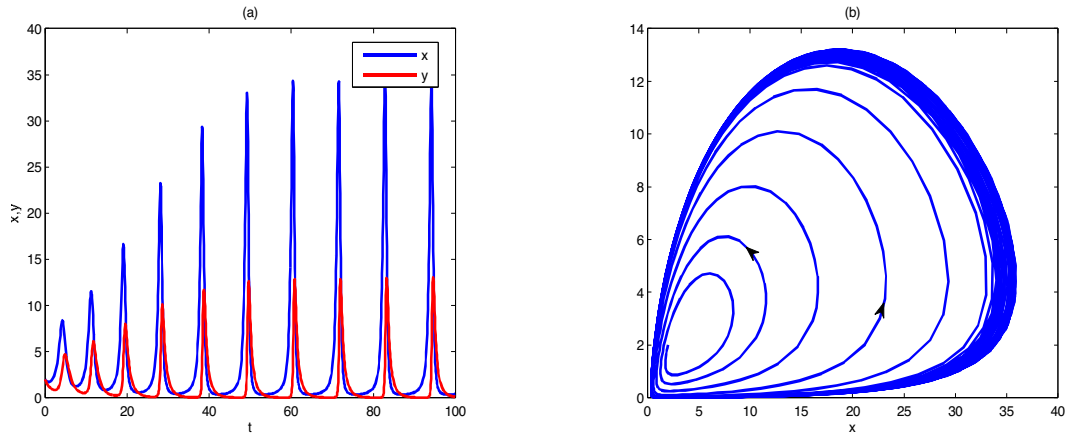

Fig. 6.8: Time series of x and y and existence of periodic solution when $\theta_w = 4.3 > \theta_w^*$.

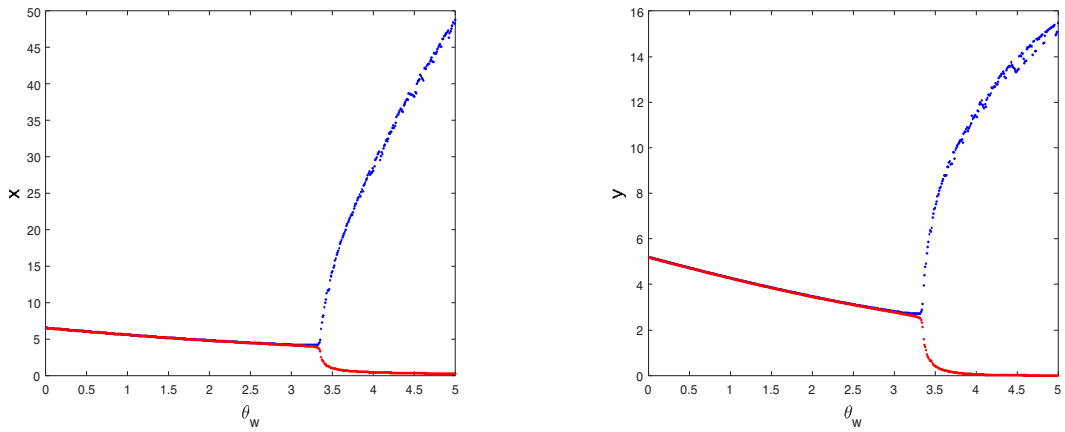

Fig. 6.9: Bifurcation diagram of the prey and predator population with respect to Allee parameter θ_w.

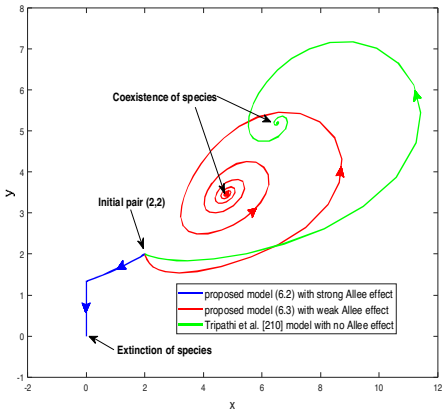

Fig. 6.10: Phase portrait of system with strong Allee effect, weak Allee effect and without Allee effect for same values of all parameters and initial conditions (2,2).

6.6.2 Delayed models

6.6.2.1 Strong Allee effect

In order to verify the theoretical predictions derived in case of delayed systems, first we simulate model (6.4), having strong Allee effect in prey population, with same values of parameters as that in (6.15). We know that introduction of delay does not affect equilibrium of the system. Thus, the interior equilibrium $E^*(6.4758, 5.1441)$ remains as it is.

For $\tau_s > 0$, we note that conditions (H_1) and (H_3) are satisfied. So, equation (6.13) has a unique positive root. Taking $i = 0$ in equation (6.14), our computer simulation yields the

following:

$$\omega_0 = 1.4472, \quad \tau_{s_0} = 0.3914,$$

and transversality condition (H_5) is satisfied. Here all three conditions of Theorem 6.4.2 hold true. Therefore system undergoes a Hopf-bifurcation at $\tau_s = \tau_{s_0} = 0.3914$. By the algorithm obtained in section 6.5, we computed the following:

$$\mu_2 = 0.0166 > 0, \quad \beta_2 = -0.0259 < 0, \quad T_2 = 0.0093 > 0.$$

This shows that the Hopf-bifurcation with respect to τ_s is supercritical, bifurcating periodic solution is stable and the period increases. Thus, the system is stable for $\tau_s = 0.16 < \tau_{s_0} = 0.3914$ which is shown in Figure 6.11. As τ_s passes through its critical value τ_{s_0}, the system loses its stability and a Hopf-bifurcation occurs into the system. In Figure 6.12(a), we have shown time series analysis for $\tau_s = 0.45 > \tau_{s_0} = 0.3914$. Figure 6.12(b) shows that a periodic solution exists and any solution trajectory initiating from inside and outside the closed trajectory, approaches towards the closed trajectory. This shows the existence of a stable limit cycle.

Bifurcation diagram has also been carried out in Figure 6.13 by taking τ_s as a bifurcation parameter. Figure makes us clear that τ_s changes the stable behavior of the system into instable behavior.

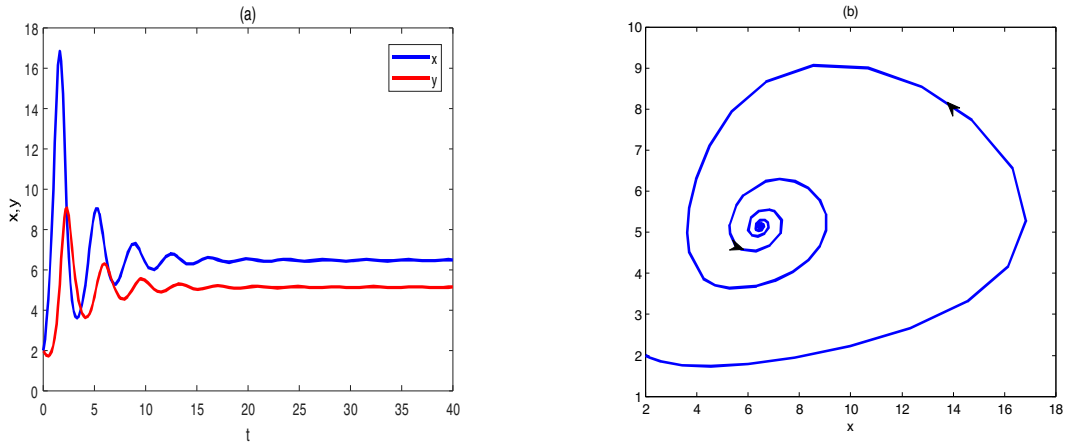

Fig. 6.11: The system (6.4) is locally asymptotically stable when $\tau_s = 0.16 < \tau_{s_0}$ other parameters are same as in (6.15).

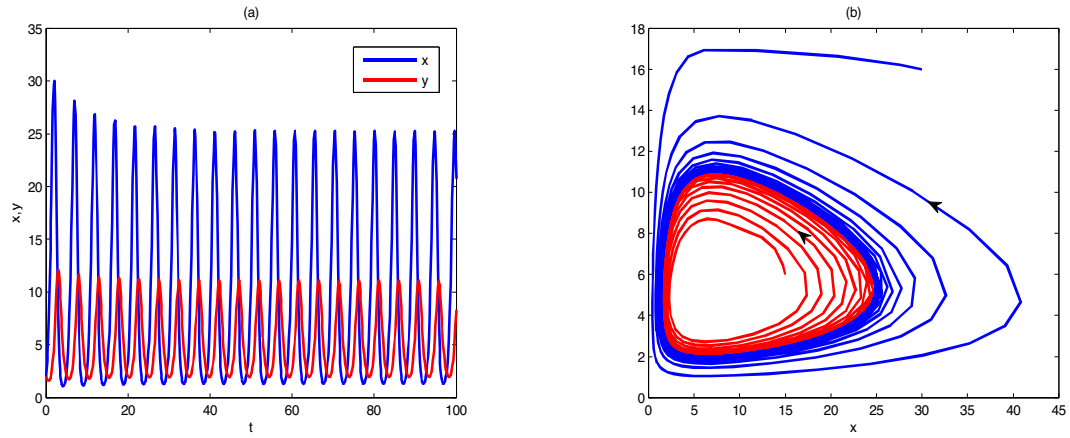

Fig. 6.12: The system (6.4) is unstable and have a periodic solution when $\tau_s = 0.45 > \tau_{s_0}$ other parameters are same as in (6.15).

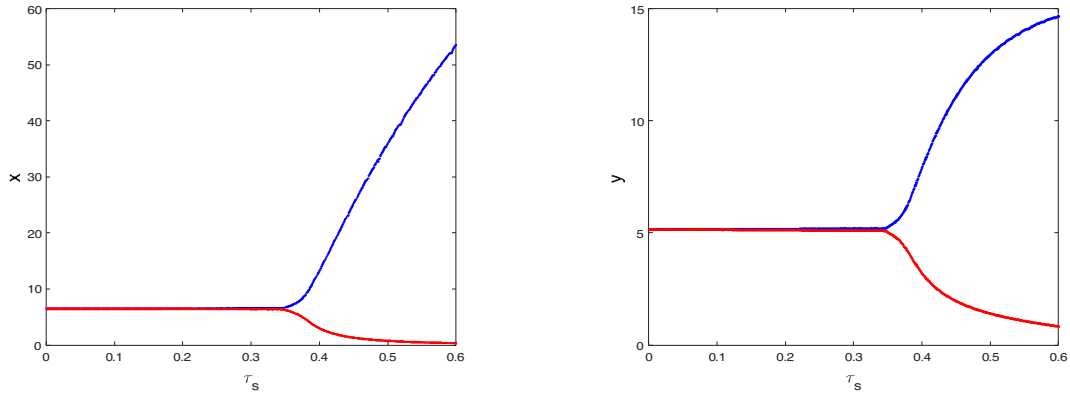

Fig. 6.13: Bifurcation diagram of the prey and predator population with respect to gestation time delay τ_s.

6.6.2.2 Weak Allee effect

The model system (6.5), with weak Allee effect in prey population has one interior equilibrium $E_*(6.4782, 5.1464)$, with set of parameters (6.15). We see that the conditions (H_1') and (H_3') are satisfied and we obtain

$$\omega_1 = 1.447, \quad \tau_{w_0} = 0.3921,$$

and transversality condition (H_5') is also satisfied. Therefore, system (6.5) undergoes a Hopf-bifurcation around interior equilibrium at $\tau_w = \tau_{w_0} = 0.3921$ (Theorem 6.4.3). Using algorithm derived in previous section, it is obtained

$$\mu_2' = 0.0281 > 0, \quad \beta_2' = -0.0437 < 0, \quad T_2' = 0.0379 > 0.$$

This shows that the Hopf-bifurcation with respect to τ_w is also supercritical, bifurcating periodic solution is stable and its period increases. Thus, the positive equilibrium E_* is asymptotically stable for $\tau_w = 0.22 < \tau_{w_0} = 0.3921$ which is shown in Figure 6.14(a) and unstable for $\tau_w = 0.48 > \tau_{w_0} = 0.3921$ (Fig. 6.14(b)). When $\tau_w = \tau_{w_0}$, system undergoes a Hopf-bifurcation at the positive equilibrium E_*. The phase portrait has been shown in Figure 6.14(b), which shows the existence of a stable limit cycle.

6.7 Conclusion

In this chapter, we made an attempt to discuss the impact of Allee effect (strong and weak both) with gestation delay in the model proposed by Tripathi *et al.* [210]. They analyzed a density dependent non-linear mathematical model (6.1). In that model, prey grows logistically and predator fully depends on prey for food that follows Crowley-Martin functional response.

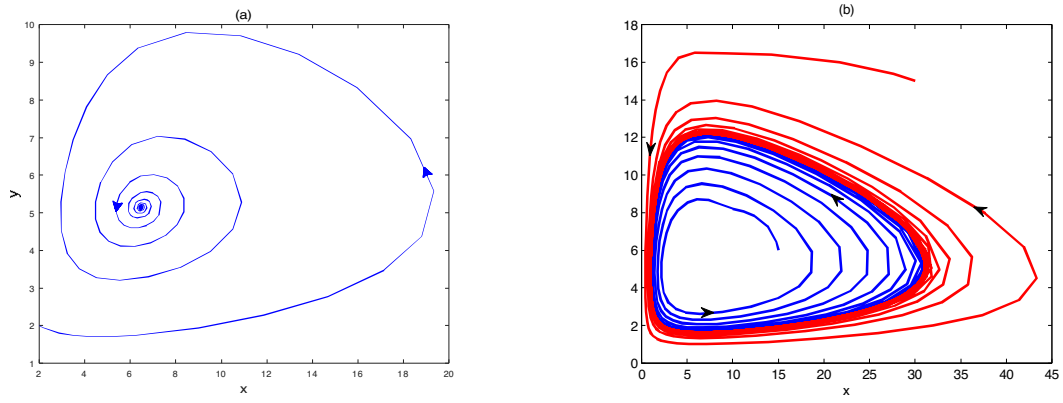

Fig. 6.14: The system (6.5) is (a) locally asymptotically stable when $\tau_w = 0.22 < \tau_{w_0}$, (b) unstable when $\tau_w = 0.48 > \tau_{w_0}$. Other parameters are same as in (6.15).

Allee effect plays an important role in the structure of population. The Allee effect increases the possibilities of extinction. Thus, we include Allee effect into model (6.1). Since, there are two types of Allee effect; strong and weak, so we studied both the models separately. In the study, we discussed positivity, boundedness of the solutions, existence of equilibrium points and their stability analysis of both the models. Positivity and boundedness of the solutions refer that the system is well behaved.

We have shown that system (6.2) and (6.3) may have more than one interior equilibrium point. Under sufficient condition (6.6) (for system (6.2)) and (6.9) (for system (6.3)) they have unique interior equilibrium point. We also derived a sufficient condition for asymptotic stability of interior equilibrium point. Then we found that model system (6.2) is bi-stable in the presence of positive equilibrium. The existence of periodic solution via Hopf-bifurcation with respect

to auxiliary parameter f in model (6.2) and Allee parameter θ_w in model (6.3) have also been shown. In Table 6.1, we presented that how the dynamics of model (6.2) differs from model (6.3). We also observed that the time of fluctuations for both prey and predator increases with increase in Allee parameter for system (6.2). But after a critical value, interior equilibrium E^* becomes unstable. In this situation system converges to stable trivial equilibrium E_0, which shows extinction of species after a critical value of Allee parameter.

Delay exhibits much more realistic behavior. The reproduction of predator after hunting prey is not instantaneous i.e. there is some time lag for gestation. Therefore to make the model biologically more realistic, we consider gestation delay for predator into both the models (6.2) and (6.3). We have analyzed Hopf-bifurcation through local stability considering delay as a bifurcation parameter. When the time delay is small then trajectory of system oscillates around the positive equilibrium for finite time and eventually settle down to equilibrium level. As the time delay increases, time of oscillations also increases and beyond a critical value of gestation delay, then stability of system switches and we obtain periodic solutions. This proves that the time delay can cause a stable equilibrium to become unstable. The stability and direction of Hopf-bifurcation also have been investigated using Normal form theory and Center manifold theory.

The numerical simulation is based on some biologically feasible data to support our theoretical results. We found that Hopf-bifurcation is supercritical and stable with increasing period. Bifurcation diagram with respect to θ_w and τ_s help us to understand about the stability behavior of the system. This chapter has some new and significant results that we hope very helpful to understanding the dynamics of prey-predator system with Allee effect and gestation delay.